

(NASA-CR-169971) CONTROL OF BONE
REMODELLING BY APPLIED DYNAMIC LOADS
Semiannual Report, Sep. 1982 - Mar. 1983
(Tufts Univ.) 18 p HC A02/MF A01 CSCL 06P

N83-19456

Unclas
G3/52 08853

Control of Bone Remodelling by Applied Dynamic Loads

NASA Grant # NAG 9-25

First Semi-Annual Report

L.E. Lanyon

&

C.T. Rubin

Department of Anatomy & Cellular Biology

Tufts University

Boston

September 1982 - March 1983



Principal Investigator - Lance E. Lanyon

Tufts University
School of Veterinary Medicine
200 Westboro Road
North Grafton, MA 01536

First semi-annual reportSummaryObjective

It is the objective of these experiments to relate the remodelling in a functionally isolated in vivo bone preparation to the characteristics of the mechanical regime to which that bone is artificially subjected.

Progress

Progress in the first six months of this grant has been substantial. The functionally isolated wing bone procedure originally used in the rooster has been adapted for the more substantial turkey ulna. This has enabled us to gain the benefit of more effective strain gauge instrumentation of the bone and longer loading life of the preparation. The isolated turkey ulna preparation has been calibrated so that it is now possible to relate accurately the strain distribution around the circumference of the bone's midshaft to the loads applied in vivo between the pins which transfix the metaphyses proximally and distally. The feedback control of the modified Instron machine used for loading in this series allows the component features of the load waveform to be varied independently. In the first series of experiments using an intermittently applied load, it has been possible to show a direct relationship between change of cross-sectional area and peak strain magnitude.

The surgical preparation of the ulna involves making two metaphyseal osteotomies, covering the ends of the bone with stainless steel caps, and transfixing these caps and the enclosed bone with Steinman pins which emerge on the dorsal and ventral surfaces of the wings. These pins are immobilized dorsally and ventrally by external fixators which are only removed when the pins are engaged in the jaws of the modified Instron machine for applied loading.

The experimental protocol requires that the course of remodelling at the ulna midshaft be correlated with the character of the mechanical regime at that location. This remodelling is the result of both the discrepancy between the naturally and artificially engendered mechanical waveform and the discrepancy between the pre-existing (natural) and artificially engendered strain distribution. In this series of experiments the difference in strain distribution is kept constant, and the artificial strain waveform varied only in terms of peak strain magnitude.

Strain recordings have been taken:

1. from the intact bone during natural wing flapping.
2. from the prepared bone during wing movement with external fixators attached.
3. from the prepared bone during external loading.

These strain recordings are obtained from three bone-bonded rosette strain gauges attached around the circumference of the bone's midshaft. Recordings from the nine strain-sensitive elements of these gauges are taken on line to a PDP 11/23 minicomputer sampling at 5 msec. intervals. Programs have been written which allow us to calculate from these raw strain data the changing magnitude and direction of the principal strains at each gauge site. These principal strains are then transformed via the material coordinate system to longitudinal strains. The gauge coordinates taken from transverse sections at the midshaft are then used so that the position and orientation of the neutral axis and the longitudinal strain magnitudes at all points around the bone's circumference may be determined.

Results

1. The magnitude and distribution of the strains around the midshaft of the intact ulna during natural loading.

The raw strain data from the three elements of one rosette strain gauge obtained during wing flapping are illustrated in Fig. 1a and the derived principal strains and their orientation from the same gauge in Fig. 1b. The magnitude and distribution of longitudinal strains are derived from these principal strain data for the three gauges around the bone's circumference. These are illustrated for the instant of peak strain on the transverse sections in Fig. 2. The value of peak strain around the bone's circumference during wing flapping was $-3300 \pm 230 \times 10^{-6}$ and the maximum strain rate was $.057 \text{ sec}^{-1}$.

2. The peak strains engendered in the prepared bone during wing movement with external fixators attached.

The pattern of strain change during wing movement with fixators attached was irregular and the peak strains achieved never exceeded 150×10^{-6} , compared to the 3300×10^{-6} achieved during wing flapping in the intact bone.

3. Strains in the prepared bone during external loading.

The calibration procedure. The load train of the modified Instron is such that the load applied by the actuator to the pins at one end of the bone is transferred through the bone's diaphysis and the pins at the other end to a load cell. It is the feedback from this load cell which the Instron matches to the command signal generated by the PDP 11/23. In order to characterize the load command signal required to produce the desired strains at the bone's midshaft, it was first necessary to determine the relationship between midshaft strain and applied load. This was done by recording the load cell feedback signal from the load cell at the same time as the raw strain data from three rosette gauges around the ulna's midshaft (Fig. 3).

Despite the compliance of the transfixing pins and the complex material properties of the bone, these calibration experiments established that a simple ramp function for the command signal was sufficient to engender a strain situation at the midshaft where the neutral axis, the points of maximum strain, and the strain rate remained constant during both loading and unloading ramps (Fig. 4).

The relationship between load and peak strain magnitude was:

$$\text{peak strain (x}10^6\text{)} = 3.8 \text{ load (Newtons)}$$

This relationship was used to predict the strain situation in the ulnas in which remodelling was assessed, and thus to which no strain gauges could be attached. In the series of experiments reported here the prime variable was to be peak strain magnitude. The strain rates during loading and release were maintained at a constant 0.01 sec.^{-1} with dwell times on and off of 0.4 sec.

Conclusions from strain gauge instrumentation of ulna midshaft

1. The strain waveform and strain distribution produced during natural and artificial loading have been accurately quantified.
2. During the period when the bones are not being loaded by the Instron machine, the ulna midshaft is subjected only to trivial strains which it is reasonable to assume have little effect on remodelling.
3. By assuming similar geometry and material properties in bones to which gauges were not attached, the strain situation at the midshaft of these bones may be predicted from the command signal to the Instron machine which, in turn, is generated by the computer.

Remodelling experiment 1. The effect on bone remodelling of peak strain magnitude.

The ulna in each bird in this experimental group was prepared in exactly the same way as that for the calibration group, except that no strain gauges were attached, and thus the bone midshaft where remodelling was to be studied was completely undisturbed. The load waveform applied to the bone, and thus the strain distribution and waveform at the midshaft, was determined by using the relationship derived from the calibration series. When each bird was to be loaded, the external fixators were removed, and following loading they were replaced. Since the strains applied to the ulna when the fixators were attached are trivial, this means that the ulna midshaft in a prepared bone is subjected only to functionally relevant levels of strain for a single period each day during which the strain waveform is unique and has been accurately characterized. The load waveform used in this experiment was the same ramped square wave used in the calibration experiment. Strain rates during loading and release were kept constant at 0.01 sec.^{-1} and the dwell times were 0.4 sec. on and off. Each bone was loaded on one occasion daily for 100 consecutive cycles, beginning on the second day postoperatively and continuing for 8 weeks. The remodelling in response to this applied load was assessed in vivo by biweekly transverse scans taken with a ^{125}I Iodine photon absorption densitometer, and postmortem by examination of sections taken from the bone at the end of the 8 week period. Single pulse doses of tetracycline were given at weekly intervals throughout the experimental period and the distribution of these dyes in undecalcified transverse sections taken from the midshaft are being used to determine the temporal sequence of the remodelling process. Histological examination of decalcified sections taken from the same location is being used to assess the details of the remodelling process including the location and thickness of bone formed or removed from around the periosteal and endosteal perimeters, the position and extent of intracortical porosis, the thickness of osteoid seams, and the tissue density of osteoblasts and osteoclasts.

1. Photon absorption densitometry.

In the series of experiments on the rooster ulna, photon absorption densitometry using ^{125}I Iodine was a valuable procedure which seemed to reflect the changes in bone mass demonstrated by histology. In the present turkey experiments this technique is not proving so reliable. The reason for this may be related to the greater amount of muscle in these animals or to some technical problems which have been plaguing the instrumentation. Due to the current uncertainty with these data, the results from this technique to date will not be presented.

2. Geometrical examination of undecalcified transverse sections.

Transverse sections 100 μ thick were cut with a diamond edged cutting wheel from the midshaft of prepared bones and their contralateral non-loaded intact pairs immediately postmortem. These sections were then mounted onto slides and their image projected onto a digitizing tablet from which the periosteal and endosteal perimeters could be traced. From these data the gross (uncorrected for porosity) area change between experimentally loaded and contralateral bones can be compared. This measure is a first order assessment of remodelling change. More detailed assessments including actual cross-sectional area change and the amount and location of new bone deposited or removed in relation to strain distribution are being developed. Progress with these measurements at present depends on our development of the microradiographic technique which we intend to use to digitize these images.

3. Histology.

Great difficulty has been encountered in obtaining adequate 5 μ thick undecalcified sections of the whole bone transverse sections. The reason why we have been attempting this is so that we can see on the same section cellular detail and distribution of fluorochromes. We have now decided to abandon this attempt and use 100 μ sections for microradiography, area

digitization and the distribution of fluorescence. Routine decalcified .
histology will be used to assess the cellular changes involved.

Results.

Change in cross-sectional area in relation to peak strain magnitude.

Eighteen ulna preparations have so far been made and successfully loaded at different peak strains for an 8 week experimental period. The results in terms of gross area change in relation to peak microstrain achieved are plotted in Fig. 5. These data show that in birds in which functional isolation is achieved and to which no loads are applied, the cross-sectional area diminishes to 85% of that on the contralateral side. (This result is similar to that achieved in the previous rooster ulna experiment.)

Daily loading which involved only 500 microstrain was insufficient to prevent this disuse osteoporosis, but above 500 microstrain, there appears to be a graded osteogenic response to increasing peak strain magnitude. The "minimum effective strain" which is associated with no change in cross-sectional area is between 1000 and 1500 microstrain. Strains higher than 1500×10^{-6} result in an increase in bone mass of up to 40% at 3000 microstrain.

Programs are being written to examine the changes in sectional properties and relate the location of the new bone formed to the change in strain distribution within the bone.

Histology.

The histology available shows that both the endosteal and periosteal new bone formed is woven in character and firmly attached to the pre-existing surface (Figs. 6 & 7). The ossification front is irregular and there are many inclusions of soft tissue being consolidated by new bone formation. There is no evidence of any delay in mineralization since the osteoid seams are narrow (Fig. 8). Quantifiable methods of analyzing these histological data are being developed. Qualitatively, however, there is no reason to

believe that the new bone formed is not normal in relation to the speed of its development.

Discussion and Conclusion.

Change in bone mass in relation to peak strain magnitude.

The demonstration of a 'dose:response curve' between strain magnitude and osteogenic response is a substantial and encouraging development. It not only demonstrates the sensitivity of the bone cell population to one very important aspect of its mechanical environment, it also establishes the minimum effective strain level required to maintain bone mass. The demonstration of such a graded response strongly supports the supposition that this response is truly strain generated rather than being a reaction to surgical trauma, irritation, etc. This establishment of a minimum effective strain is of considerable importance to the problem of maintaining bone mass in a non-gravity environment. The strain situation in the prepared ulna is totally different from that induced during natural wing loading yet 100 cycles per day of a load which engendered strains of $1000-1500 \times 10^{-6}$ were sufficient to prevent bone loss. It remains to be determined whether the minimum effective strain demonstrated in this experiment is a characteristic of the particular strain distribution we employed or whether this level of strain will prevent bone loss regardless of its distribution.

Summary of Progress

The protocol has been established for producing a unique, controllable, and accurately defined strain regime in a bone otherwise deprived of functional loading. Preliminary analysis of the data demonstrates a graded osteogenic response to increased strain magnitude. Procedures to analyze these remodelling data in greater detail are being developed. Experiments to determine the effect of rate of change of strain have been started.

Publications

The data in this report will be presented to the 1983 Meeting of the Orthopaedic Research Society and will appear in the Proceedings of that meeting and subsequently in Orthopaedic Transactions.

gauge 1

gauge 2

gauge 3

ORIGINAL PAGE IS
OF POOR QUALITY

Fig. 1a. Recordings taken during wing flapping from the 3 separate strain sensitive elements of one of the 3, 45° rosette strain gauges placed around the midshaft of the intact ulna.

principal
tensionprincipal
compressionorientation
 θ

Fig. 1b. The principal tension and compression strains (ξ_t & ξ_c) and their orientation θ for one rosette gauge site derived from the raw strain data in Fig. 1a. The principal strain data from each of the 3 rosette gauge sites are transformed to longitudinal strains and used to predict the strain distribution around the bones' circumference.

ORIGINAL PAGE IS
OF POOR QUALITY

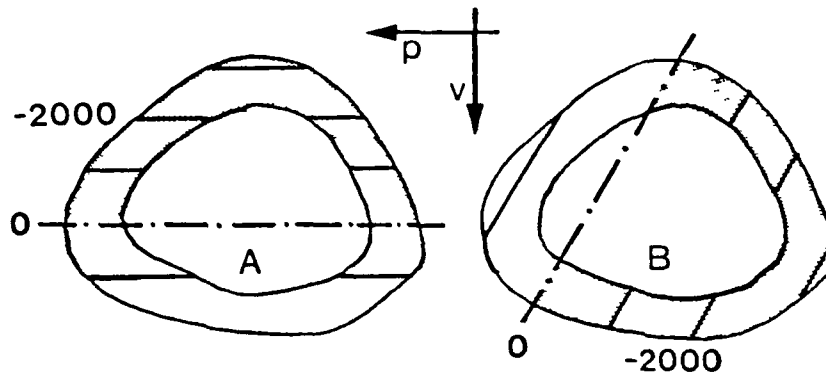
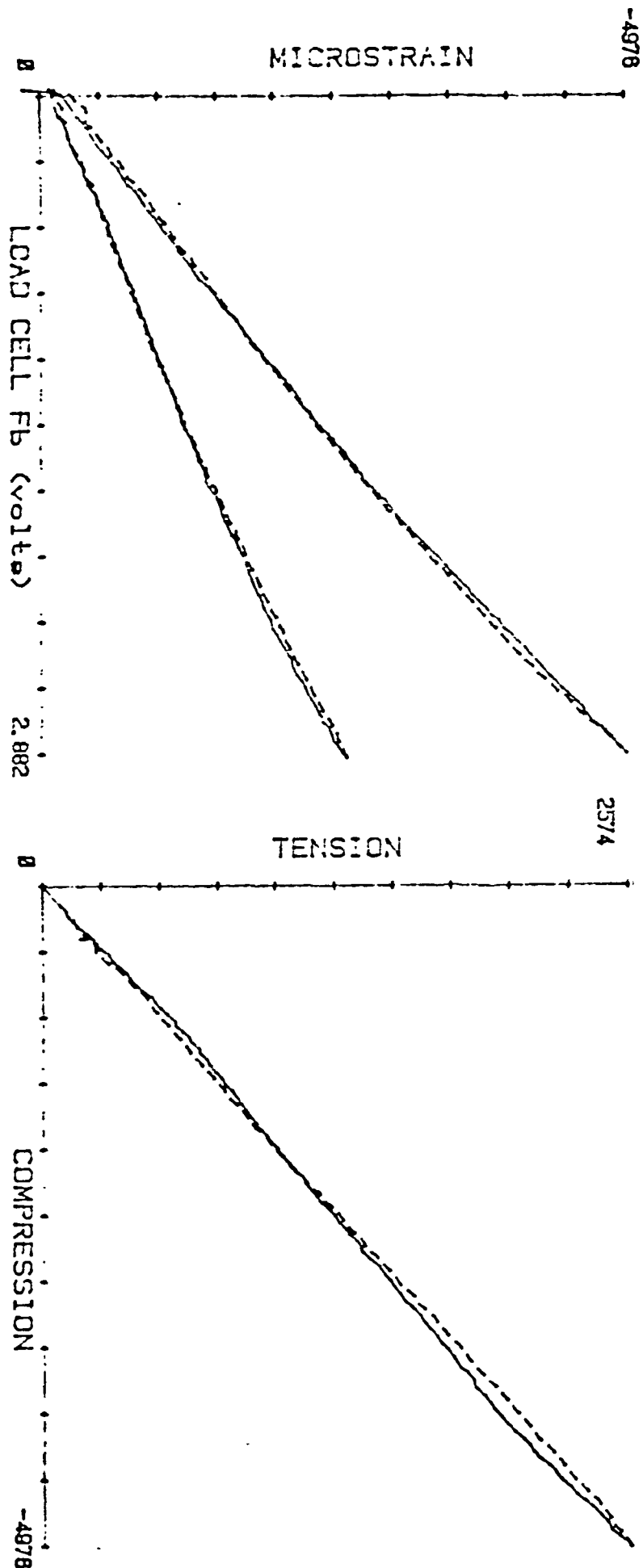


Fig. 2. The longitudinal strain distribution of the intact turkey ulna during flapping (A), and the floating ulna preparation (B) during applied loading. Although, in this case, the capped ulna is loaded to $-3300 \mu\text{E}$, the same level as that elicited during vigorous functional activity in the intact bone, the neutral axis (broken line) has shifted by 120 degrees. Each solid line represents an increment of $1000 \mu\text{E}$.

ORIGINAL PAGE IS
OF POOR QUALITY

13



HENAGA, UCL 2/9/82

load vs. tension = $72.33 + 829.148x$; .9986
load vs. comp. = $-71.26 + -1656.12x$; -.999
comp. vs. tension = $36.71 + -.501x$; -.9997

HENAGA, DCL 2/9/82

load vs. tension = $60.04 + 818.355x$; .9983
load vs. comp. = $-122.38 + -1553.59x$; -.9982
comp. vs. tension = $-4.12 + -.527x$; -.9999

Fig. 3. Plot of a calibration run on a prepared ulna loaded to 1300 newtons, causing a peak of -5000 microstrain. The plots of peak tension and compression are given as a function of the load cell output (left), and the relationship of tension to compression (right). The loading ramp is the solid line, unloading ramp is the broken line.

ORIGINAL PAGE IS
OF POOR QUALITY

ORIGINAL PAGE IS
OF POOR QUALITY

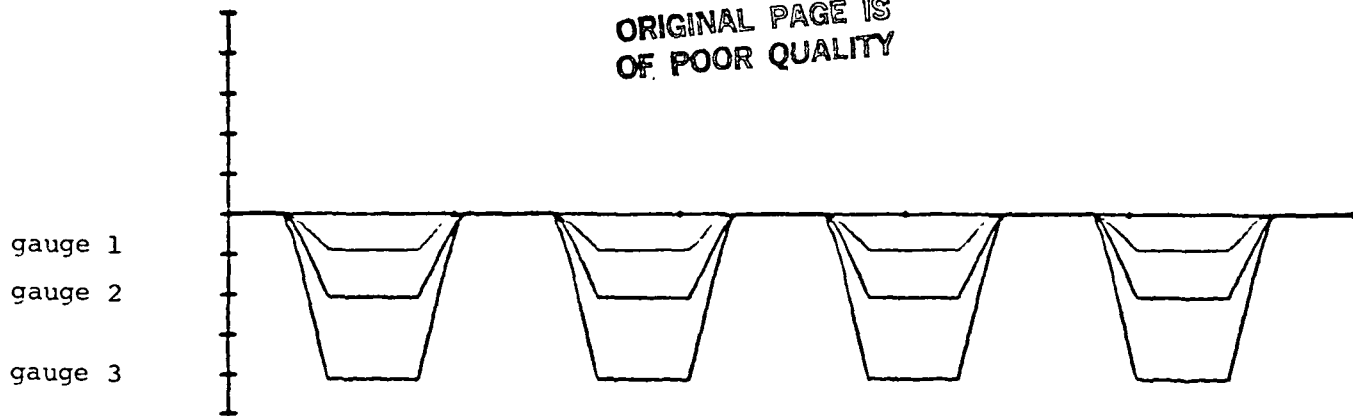


Fig. 4a. Similar recordings to those in Fig. 1a only taken from one rosette gauge during loading by the Instron machine.

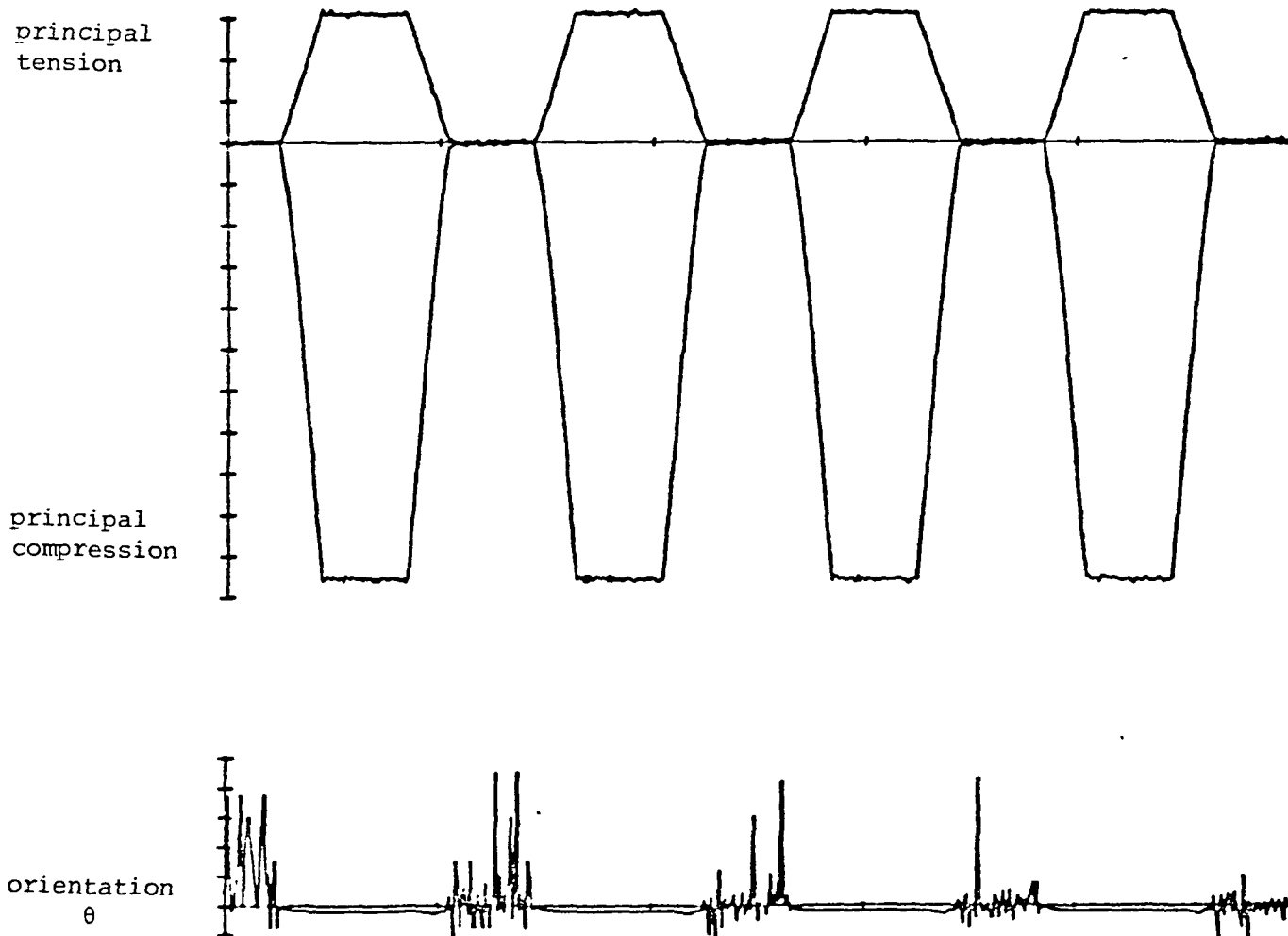


Fig. 4b. The principal tension and compression strains and their orientation derived from the raw strain data in Fig. 4a.

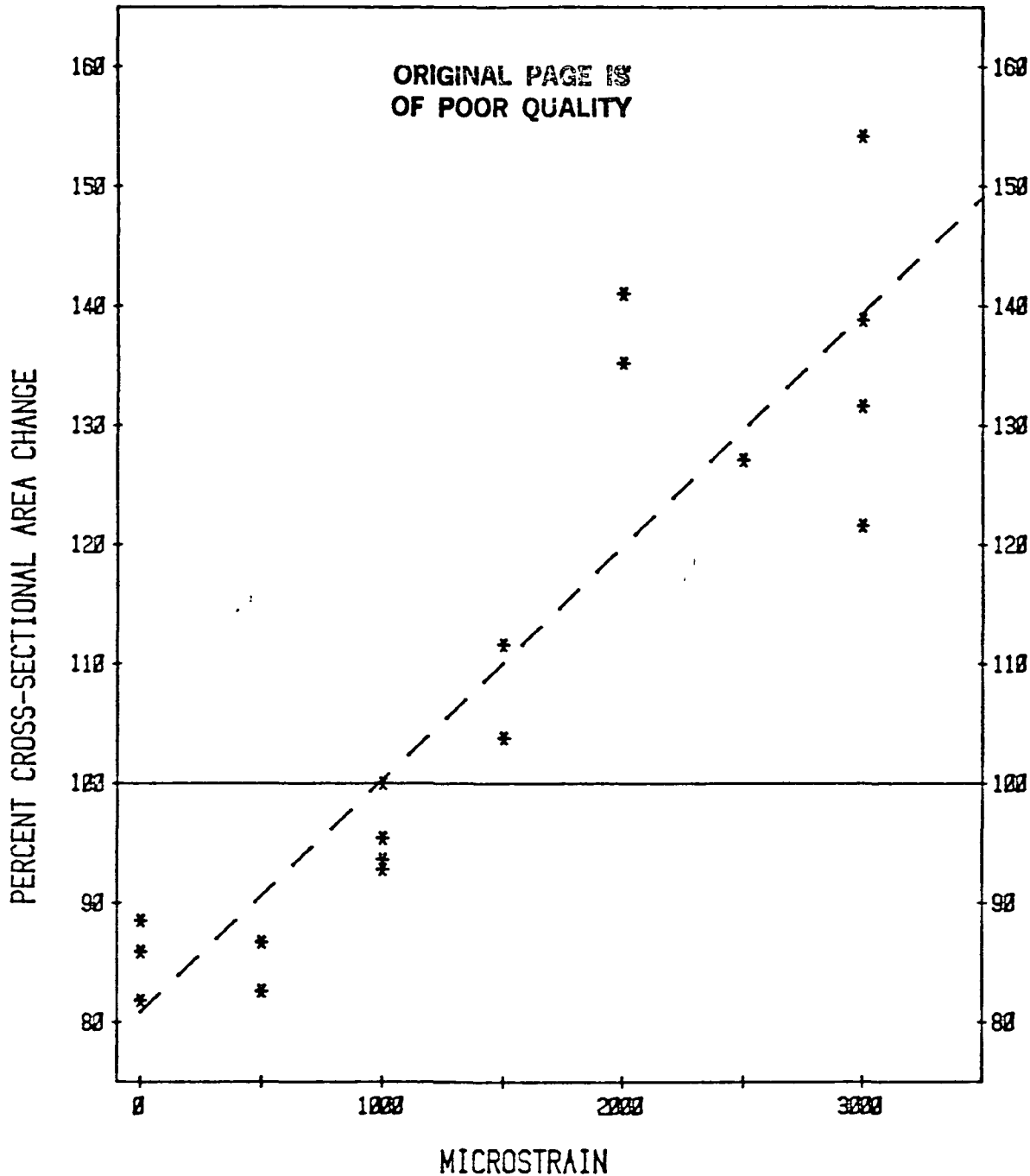


Fig. 5. The percentage difference in midshaft cross-sectional area between prepared and contralateral intact ulnae plotted against the peak strain magnitude engendered during 100 consecutive cycles of external loading. The line fitted to the data points in this figure is a linear regression ($y = 0.19x - 19.15$) with an r value of 0.91, ($n = 18$). The x intercept is equivalent to the minimum effective strain and using this linear fit is equal to 982×10^{-6} .

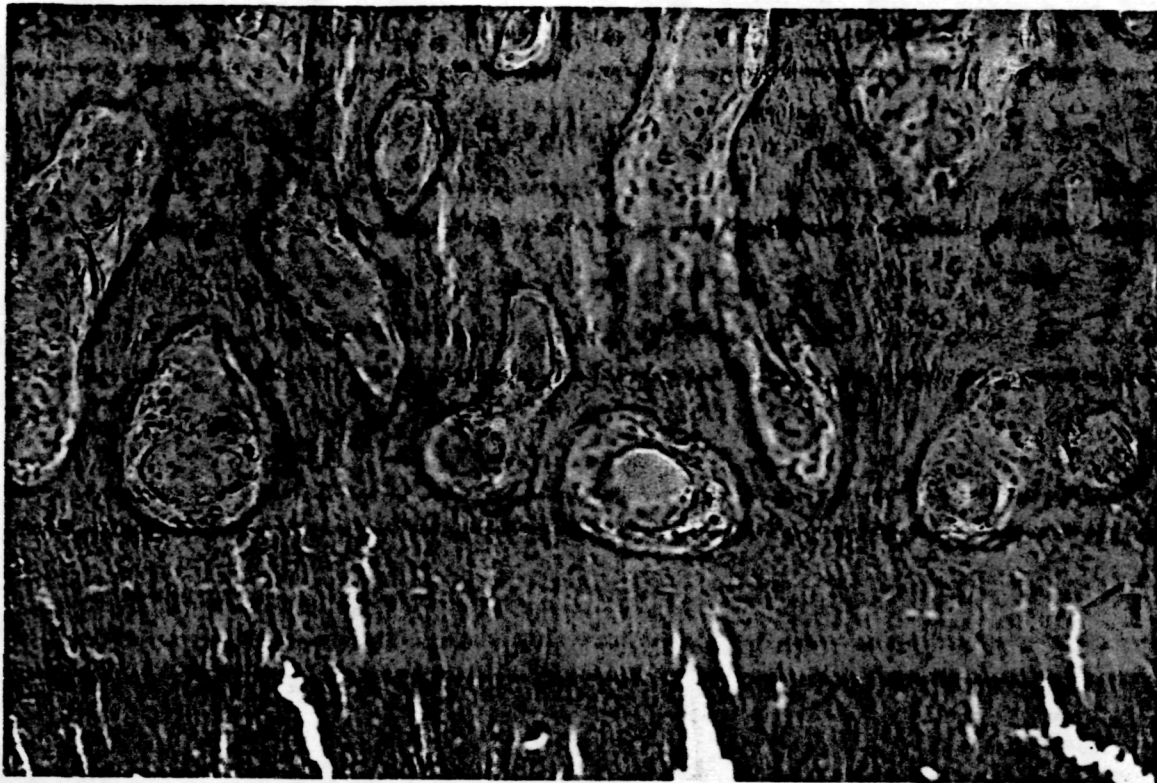


Fig. 6. A low power photomicrograph of an undecalcified 5 μ thick bone section to show new subperiosteal bone formation. The junction between pre-existing and new bone is evident (arrowed). The new bone is woven in character and the periosteal outline irregular. **ORIGINAL PAGE IS OF POOR QUALITY**



Fig. 7. Microradiograph of a 100 μ thick section showing a similar junction between new bone formation and the pre-existing periosteal surface showing the good mineralisation of the new bone.

ORIGINAL PAGE IS
OF POOR QUALITY



Fig. 8. A photomicrograph at higher power of the periosteal ossification front in Fig. 6. The ossifying surface can be seen to be covered with osteoblasts and the osteoid seam is narrow showing no evidence of delayed mineralisation.